Available online at www.sciencedirect.com
ScienceDirect
Journal of Power Sources 160 (2006) 1204–1210
JOURNAL OF POWER SOURCES
www.elsevier.com/locate/jpowsour

# A polyvinyl alcohol/*p*-sulfonate phenolic resin composite proton conducting membrane

Chien-Shun Wu [a], Fan-Yen Lin [a], Chih-Yuan Chen [b], Peter P. Chu [a,*]

[a] *Deparment of Chemistry, National Central University, Chung-Li 32054, Taiwan*
[b] *Material Research Laboratory, Industrial Technology Research Institute (ITRI), Hsin-Chu, Taiwan*

Received 26 November 2005; received in revised form 10 March 2006; accepted 10 March 2006
Available online 9 May 2006

**Abstract**

Membranes composed of poly(vinyl alcohol) (PVA) and a proton source polymer, sulfonated phenolic resin (s-Ph) displayed good proton conductivity of the order of $10^{-2}$ S cm$^{-1}$ at ambient temperatures. Upon cross-linking above 110 °C, covalent links between the sulfonate groups of the phenolic resin and the hydroxyl groups of the PVA were established. Although this sacrificed certain sulfonate groups, the conductivity value was still preserved at the $10^{-2}$ S cm$^{-1}$ level. In sharp contrast to Nafion, the current membrane (both before and after cross-linking) was also effective in reducing the methanol uptake where the swelling ratio decreased with increase of methanol concentration. Although both the methanol permeation and the proton conductivity were lower compared to Nafion, the conductivity/permeability ratio of 0.97 for the PVA/s-Ph is higher than that determined for Nafion. The results suggested the effectiveness of proton transport in the polymer-complex structure and the possibility that a high proton conductivity can be realized with less water.


*Keywords:* Fuel cell; Membrane; Cross-linking; Acid–base complex; Methanol cross-over

## 1. Introduction

The proton exchange membrane is a key component in devices such as the hydrogen fuel cell and the direct methanol fuel cell (DMFC), where high proton conductivity is the primary goal. However, preserving other membrane properties such as chemical stability in the acidic environment, low methanol crossover (<$10^{-7}$) at high methanol concentration, low swelling in presence of methanol and good mechanical properties are also vital issues to be addressed.

As widely accepted, proton conductivity in an aqueous environment is achieved primarily by the structural relaxation of the hydrogen bonding network as well as the self-diffusion of the charged hydronium clusters [1]. A growing number of studies indicate that translocation between adjacent proton defects can also lead to good proton conductivity [2]. In general, the overall conductivity is dependent on the degree of water uptake and the channel structures of the membrane where both mechanisms are active. This subject has been thoroughly discussed in a recent review by Kreuer [3]. In the situations where membrane displayed a large solvent uptake, the possibility of excessive swelling led to the deterioration of the membrane mechanical properties. In addition, a high electrolyte concentration could reduce proton mobility due to solvent dragging. Therefore, it is highly desirable to tailor the proton-conducting environment in the membrane such that high proton conductivity can be established with a minimal amount of the aqueous solvent.

Acid–base pairing is one plausible approach by which high ionic conductivity can be realized in the presence of low humidity. The use of the base molecule as a solvent for acidic protons in the polymer or in the acidic liquid has elevated the proton conductivity due to the creation of protonic defects as well as mobility in this small molecule solvated system [4–6]. Savinell and co-workers showed that the addition of $H_3PO_4$ to (polybenzylimidazole) PBI delivered appreciable proton conductivity at elevated temperatures under non-aqueous conditions [7,8]. Recently, it was demonstrated that the ordered flow channel created by low molecular weight acid/base oligomers delivered a more favorable proton conduction behavior compared to the

* Corresponding author. Tel.: +886 3 425 8631; fax: +886 3 422 7664.
*E-mail address:* pjchu@cc.ncu.edu.tw (P.P. Chu).

0378-7753/$ – see front matter © 2006 Published by Elsevier B.V.
doi:10.1016/j.jpowsour.2006.03.038

situations when such pairing was absent [9,10]. In the non-aqueous condition, proton conductivity reached $\sim 10^{-3}$ S cm$^{-1}$ above 100 °C. However, such materials suffered severely from leaching of the small acid/base molecules in the presence of the methanol solvent. Kerres et al. has also demonstrated that blending of two or more polymers with acid and base functionality to form a composite membrane is one approach to achieve the goal [11–15].

The present paper extends the acid and base polymer blend concept by using a weak base polymer, poly(vinyl alcohol) (PVA) (**1**) (see below) with an acid source sulfonated phenolic resin (s-Ph) (**2**). As the proton is shared between the sulfonate group and the hydroxyl (weak base) of PVA forming a hydrogen bonded network, the acid–base pairing can lead to short range ordered domains thus creating a highly directional proton flow channel. Specifically for the present case, a covalent bond is formed between the s-Ph and PVA moiety when the blend is dehydrated at elevated temperatures, which increases the membrane strength. The cross-linked membrane displayed a strong self-standing property but does not suffer from loss of proton conductivity. Most importantly, the membrane shows decreased solvent uptake and reduced swelling with increasing methanol concentration, which can be advantageous for the application in direct methanol fuel cells (DMFC).

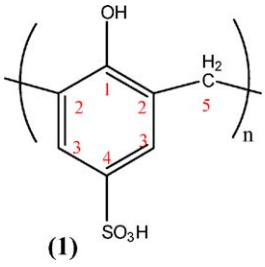


(1)

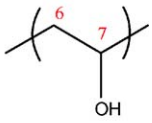


(2)

## 2. Experimental

### 2.1. Membrane preparation

The membranes used in the present study were prepared by a solvent-cast method. Poly(vinyl alcohol) (PVA) [MW = 80,000, SHOWA], phenol-4-sulfonic acid solution [Fluka, Germany], 37% formaldehyde solution [UCW, Taiwan], dimethyl sulfoxide (DMSO) [TEDIA, USA] were used as received. The phenol-4-sulfonic acid and formaldehyde were used in a 1:1 mole ratio for the formation of sulfonated phenolic (s-Ph) resin by following the procedure described in the literature [16]. The appropriate wt.% of PVA and s-Ph were weighted respectively and then dissolved under agitation in DMSO at 80 °C. After that, homogeneous solutions were poured onto Teflon dishes to fabricate the film by drying at 80 °C in a vacuum oven. The final products were in the form of films with thicknesses of 300–400 μm. The dried membranes were heated for 2 h in a vacuum oven at the desired temperature (herein termed "curing "), i.e. 110, 130 and 150 °C, respectively. These films were stored under a dry argon environment prior to use.

### 2.2. Membrane characterization

The coordination structure was investigated using infrared (IR) spectroscopy on KBr using a BIO-RAD FT-IR spectrometer [FTS-155]. The microstructure of the membranes was determined with a Varian 400 MHz solid-state NMR spectrometer. A Perkin-Elmer TGA-7 series, was used to record TGA measurements in the range of 30–900 °C. The weights of the samples were maintained in the range of 3–5 mg.

### 2.3. Water uptake and solvent uptake

Membrane samples were immersed in distilled water or different concentrations of methanol and heated at 60 °C for 2 h. Then samples were dried in a vacuum oven at 80 °C overnight and weighed. The uptake was calculated using the follow equation [17]:

$$\text{uptake} = \frac{W_{\text{wet}} - W_{\text{dry}}}{W_{\text{dry}}} \times 100\%$$

where $W_{\text{wet}}$ is the weight of the dry membrane and $W_{\text{dry}}$ corresponds to the weight of the membrane soaked in water or methanol (g), respectively.

### 2.4. Ion exchange capacity (IEC)

The ion exchange capacity (IEC) of the membranes was evaluated using a titration method [17]. The stored membranes in an argon environment were immersed in 1 M NaCl solution and stirred for 6 h at 40 °C. The protons released during the ion exchange process were titrated with a 0.01N NaOH solution. NaOH solution was titrated with potassium hydrogen phthalate (KHP) prior to use.

### 2.5. Proton conductivity measurement

The proton conductivity of these membranes were investigated with a cell consisting of two stainless steel electrodes over the frequency range 1 MHz to 1 Hz, using frequency analyzer AUTOLAB/PGSTAT 30 electrochemical instrument. The bulk resistance ($R_b$) was determined from the equivalent circuit analysis by using a frequency response analyzer (FRA software). The conductivity values ($\sigma$) were calculated by the equation, $\sigma = (1/R_b)(t/A)$, where $t$ is the thickness and $A$ is the area of the sample.

### 2.6. Methanol permeability measurement

The methanol permeability of the membranes were performed in a permeation measuring device [18]. The membrane (6 cm$^2$) was inserted between vessels A and B. A volume of 40 ml methanol solution (50 vol.%) and 40 ml deionized water was placed in each vessels A and B, respectively. After a fixed period of time, the amount of methanol that crossed through the membrane and diffused to the vessel B was determined by refractive index [ATAGO3T], comparing to a methanol concentration calibration curve.

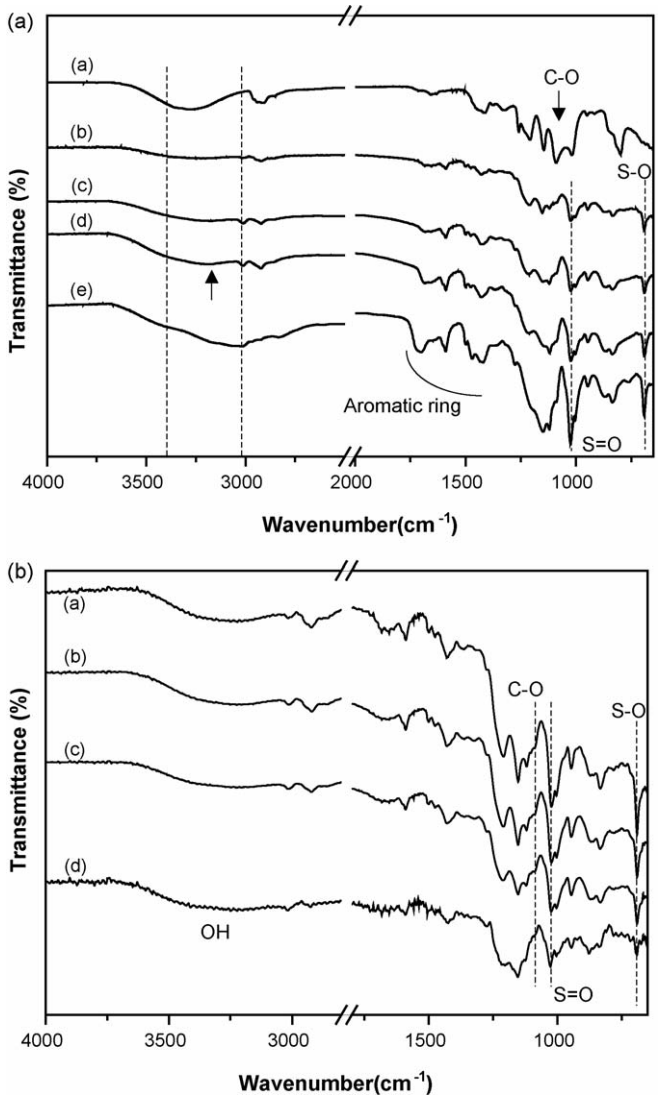


Fig. 1. (a) FT-IR spectra of (a) pure PVA, (b) 40, (c) 60 and (d) 80 wt.% s-Ph in PVA and (e) pure s-Ph. (b) FT-IR spectra of PVA60SP samples cured at (a) 80, (b) 110, (c) 130 and (d) 150 °C.

## 3. Results and discussion

The main issues to be examined in the membranes composed of s-Ph and PVA are: (1) the degree of cross-linking as a function of curing temperature and s-Ph composition, (2) the change of proton conductivity as a function of ion exchange equivalent (IEC), and solvent uptake for various s-Ph compositions, and (3) the effects of cross-linking to the methanol permeability and proton conductivity.

FTIR studies were carried out on samples containing PVA and s-Ph blends (Fig. 1a), and on samples cured at different temperatures (Fig. 1b). Fig. 1a displays the FT-IR spectra of pure PVA (a), and samples containing 40 (b), 60 (c) and 80 wt.% (d) of s-Ph and the parent s-Ph (e). In pure PVA, we observed a doublet peak around 1000–1300 $cm^{-1}$ and a broad region around 3000–3500 $cm^{-1}$. They are characteristic of PVA and have been assigned to C–O stretching and O–H stretching, respectively. In pure s-Ph, two peaks at 1030 $cm^{-1}$ and around 700 $cm^{-1}$ have been assigned to S=O and S–O symmetric stretching, respectively. Upon blending s-Ph with PVA, the S=O and S–O stretching characteristic of s-Ph grows while the C–O stretching characteristic of PVA decrease. The O–H stretching region in s-Ph displayed two peaks, which have previously been identified as hydrogen bonded OH (~3100 $cm^{-1}$) and non-hydrogen bonded free –OH (~3400 $cm^{-1}$) [19]. It is known that hydrogen bonding is the primary driving force for the miscibility between PVA and phenolic resin [19]. With the presence of the sulfonate group on the phenolic, inter-molecular hydrogen bonding, is expected to increase and the miscibility between the two polymers would be even better. However, the region from 3000 to 3500 $cm^{-1}$ contains information from a multitude of hydrogen bond associations between the aromatic sulfonate and the hydroxyl group of the PVA and within the s-Ph and within the PVA moieties, and so it is too broad to allow for unambiguous quantification. Nevertheless, a gradual shift of the PVA –OH (located at ~3300 $cm^{-1}$), towards ~3100 $cm^{-1}$ of the hydrogen bonded OH is evident with increasing s-Ph content as indicated by the arrow in Fig. 1a. More direct evidence of the inter-molecular hydrogen bonding comes from solid-state NMR studies, as will be discussed later.

Curing the sample leads to changes in these features. Fig. 1b displays change in FTIR spectra of the PVA60SP samples cured at different temperatures. Negligible changes are found in the O–H band region but intensities of S=O and S–O peaks decrease with increasing annealing temperature. The reduced $SO_3$ signals suggested aromatic de-sulfonation or cross-linking between the $SO_3$ groups of the phenolic resin and the hydroxyls of PVA might take place. Although possible, substantial de-sulfonation was not occurring until the temperature was raised to above 150 °C [20]. As evident in Fig. 1b, after annealing sample at 150 °C the $SO_3$ concentration dropped substantially from the original value prior to heating.

The miscibility and the hydrogen bonding between s-Ph and PVA is best illustrated by the $^{13}C$ solid-state NMR cross-polarization dynamics. The $^{13}C$ NMR spectra for samples containing 40 and 60 wt.% s-Ph at different contact times are summarized in Fig. 2. The relationships between the magnetization intensity and cross-polarization contact time can be described by the following equation:

$$M(t) = \frac{M_0 \left[ \exp\left(\frac{-t}{T_{1\rho}^{H}}\right) - \exp\left(\frac{-t}{T_{CH}}\right) \right]}{\frac{1-T_{CH}}{T_{1\rho}^{H}}}$$

By this analysis, the cross polarization time $T_{CH}$ and the proton relaxation time in the rotating frame $T_{1\rho}$ can be derived independently, and the results are summarized in Table 1. The $T_{CH}$ for carbon directly attached to the sulfonic acid group ($\delta$ = 128 ppm), increases when the s-Ph concentration increases from 40 to 60 wt.%. Similarly, $T_{CH}$ for the methine carbon attached to the hydroxyl group ($\delta$ = 68 ppm) shows the reverse trend. The increase of $T_{CH}$ is known to be associated with the reduction of dipolar interaction between carbon and hydrogen nuclei, which can originate either from a lengthening carbon hydrogen distance or from an increasing molecular re-orientation. Since the

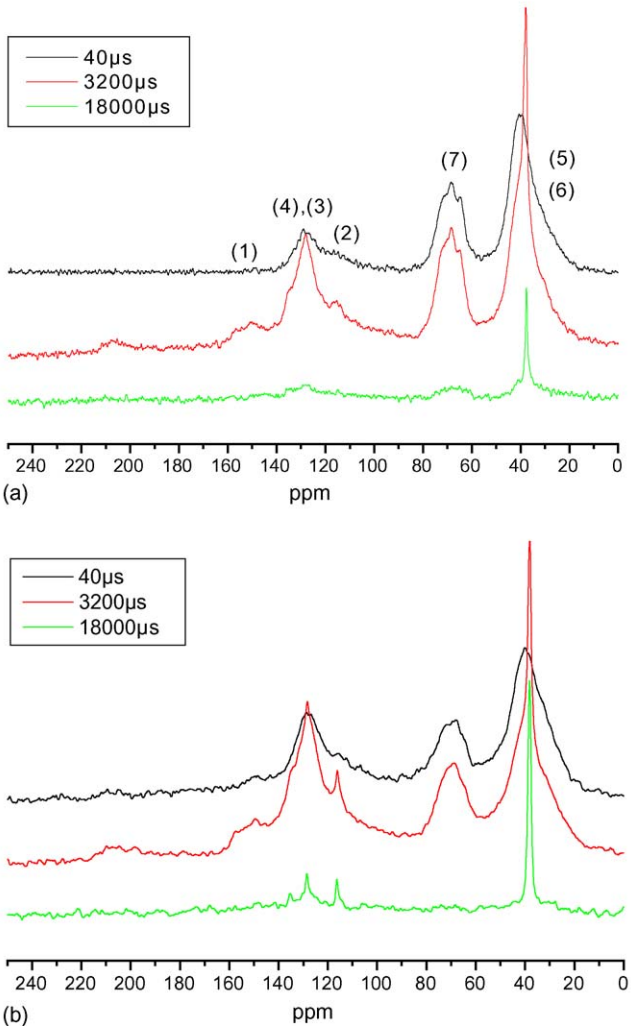


Fig. 2. (a) The $^{13}C$ solid-state NMR spectra of PVA/40 wt.% s-Ph at different contact times. (b) The $^{13}C$ solid-state NMR spectra of PVA/60 wt.% s-Ph at different contact times.

Table 1
Cross-polarization dynamics for the individual carbons as indicated in structure (**1**) and (**2**) in PVA40SP and PVA60SP

| Peak number | ppm | $T_{CH}$ (μs) | |
|---|---|---|---|
| | | PVA40SP | PVA60SP |
| 2 | 116 | – | 478 |
| 3, 4 | 128 | 695 | 444 |
| 5, 6 | 38 | 3279 | 2989 |
| 7 | 68 | 331 | 408 |

CH is fixed due to covalent nature, the decrease in $T_{CH}$ is thus gauging the decrease of the molecular motion. The results therefore, suggest a rise of motion in the s-Ph moiety and a restriction of molecular reorientation in the PVA segment upon blending. The two moieties must be in close proximity with intimate miscibility in order to produce the observed effect. A plausible acid–base interaction between PVA and s-Ph is depicted in Scheme 1 where bi-functional hydrogen bonding is established between s-Ph and PVA.

This structure does not include the configurations of the intramolecular hydrogen bonding within s-Ph and within PVA.

Fig. 3 shows the IEC and conductivity values for samples containing a different wt.% of s-Ph. Both IEC and conductivity increase with increasing s-Ph content. Notice that the IEC value approaches 3.0 mmole $g^{-1}$ with the conductivity reaching nearly $10^{-1}$ S $cm^{-1}$ for pure s-Ph. The proton conductivity is highly correlated with the increase of the sulfonate group. Notice that the conductivity at high IEC values does not taper off, as was the case found in most proton conducting membranes, which suggests the majority of sulfonate groups are fully accessible to water.

Cross-linking of the matrix by annealing the sample altered both the IEC and proton conductivity. Both properties are displayed in Fig. 4 for membranes (PVA60SP, 60 wt.% s-Ph) cured at temperatures 110, 130 and 150 °C. The changes are relatively

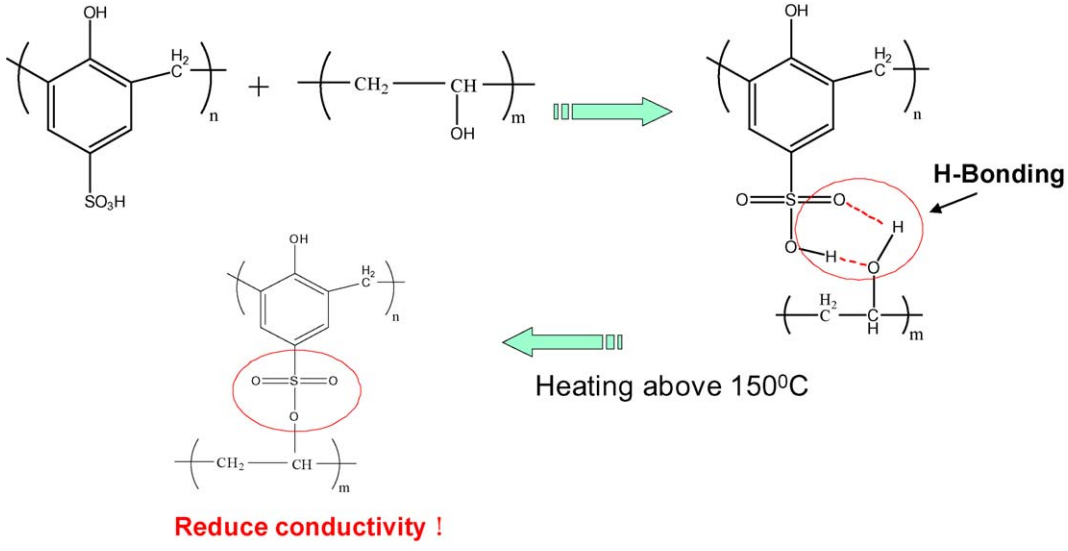


Scheme 1. The probable acid–base interactions between PVA and s-Ph.

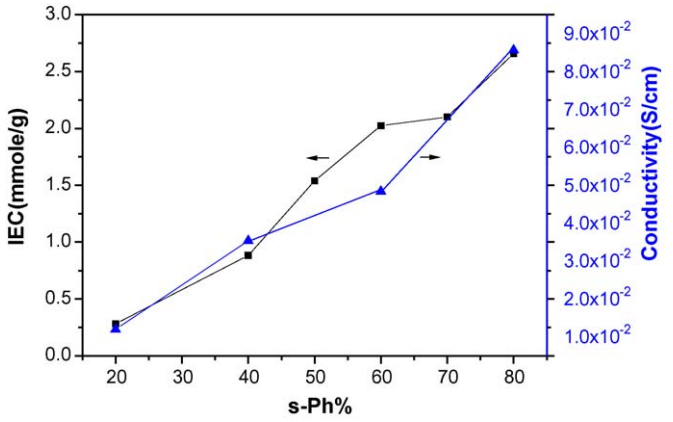


Fig. 3. Ion exchange capacity (IEC) and conductivity at different wt.% of s-Ph in PVA polymer.

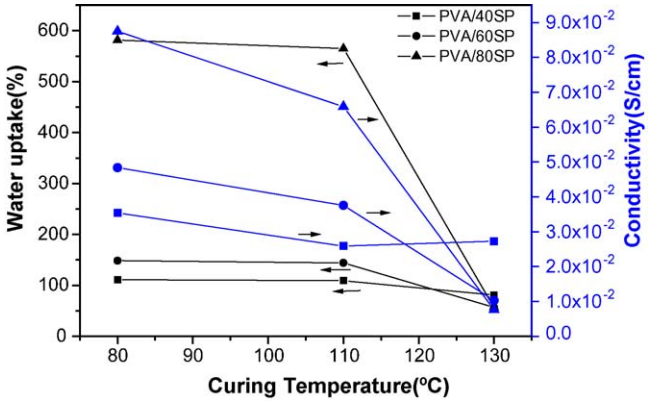


Fig. 5. Water uptake and proton conductivity as a function of curing temperature for samples of different composition.

small below 110 °C, but a significant drop is found when the curing temperature is raised above 130 °C. From ambient temperature to 130 °C the IEC dropped from 2.0 to 1.5 mmole $g^{-1}$, consistent with the drop of the $SO_3$ concentration, measured from the IR. However, the conductivity dropped more to well below the $10^{-2}$ S $cm^{-1}$ level after annealing at 130 °C. Similarly, the IEC value of the sample PVA60SP cured at 150 °C is located in between that of PVA20SP and PVA40SP, but its conductivity does not reflect the fair IEC value and shows two orders less conductivity. The significance of the fact that the IEC remains high but the conductivity becomes much lower suggests that local motion, especially the degree of free re-orientation of the sulfonate group is critical to proton transfer. Manipulating this polymer microstructure, which can either create more fluent conducting channel connectivity or increases the $-SO_3$ free reorientation are other means to be exploited to improve the conductivity. The conductivity and IEC values for other samples of different amount of s-Ph are summarized in Table 2.

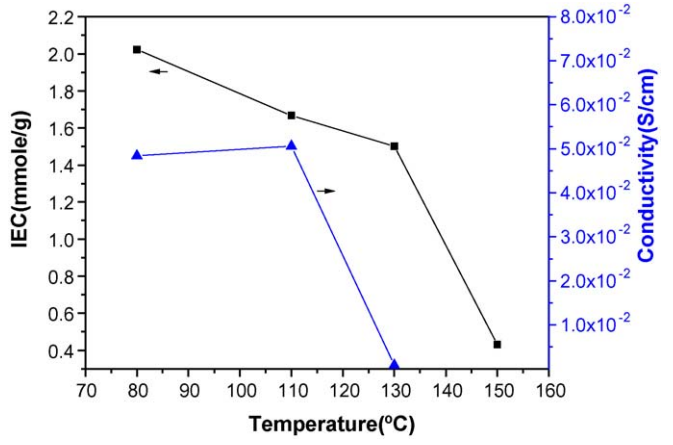


Fig. 4. Ion exchange capacity (IEC) and conductivity of PVA60SP samples cured at different temperature.

The amount of solvent that was required to initiate proton transport served to measure the efficiency of the membrane in terms of proton transport. Fig. 5 shows the water uptake as a function of the curing temperature for samples containing a different wt.% of s-Ph. For comparison, the conductivity data are also included. It is clear that as the curing temperature is increased, the water uptake decreases and the conductivity decreases also. The change is small, but when the temperature is increased to 130 °C, a substantial decrease both in the conductivity and water uptake are observed. Possible reasons for this are: (1) the reduction of $SO_3$ due to the formation of a covalent cross-linking sulfonate ester structure (see Scheme 1) between *p*-s-Ph and PVA and (2) the loss of $SO_3$ concentration due to disintegration of $SO_3$ at temperatures above 130 °C. The second possibility can be ruled out since the IEC values are not decreased before a substantial drop of conductivity is observed. Furthermore, independent thermal gravimetric analysis showed that de-sulfonation does not occur until 150 °C.

Table 2
The IEC, water uptake, λ and proton conductivity for various PVA/s-Ph compositions

| Samples | Curing temperature (°C) | IEC (mmole $g^{-1}$) | W.U. (%) | λ ($nH_2O/SO_3^-$) | Conductivity (S $cm^{-1}$) |
|---|---|---|---|---|---|
| PVA | – | – | – | – | $5.92 \times 10^{-5}$ |
| PVA20SP (17:1)* | – | 0.28 | 50.17 | 98.33 | $1.20 \times 10^{-2}$ |
| PVA40SP (6:1) | – | 0.88 | 113.67 | 71.55 | $3.54 \times 10^{-2}$ |
| PVA50SP (4:1) | – | 1.54 | 160.62 | 57.95 | $5.26 \times 10^{-2}$ |
| PVA60SP (3:1) | – | 2.02 | 173.91 | 47.75 | $4.84 \times 10^{-2}$ |
| PVA60SP | 110 | 1.67 | 121.93 | 40.66 | $3.76 \times 10^{-2}$ |
| PVA60SP | 130 | 1.50 | 49.85 | 18.44 | $8.59 \times 10^{-4}$ |
| PVA80SP (1:1) | – | 2.66 | 366.2 | 76.55 | $8.57 \times 10^{-2}$ |
| SP | – | 3.10 | – | – | $1.97 \times 10^{-1}$ |

* The parenthesis is the monomer ratio between vinyl alcohol vs. phenol-4-sulfonic.

Table 3
Permeability and the $\sigma/D$ value of PVA/SP membranes

| Samples | Curing temperature (°C) | Methanol permeability ($cm^2\ s^{-1}$) | $\sigma/P$ ($\times 10^4$) |
|---|---|---|---|
| PVA20SP | – | $1.81 \times 10^{-6}$ | 0.66 |
| PVA20SP | 110 | $7.19 \times 10^{-7}$ | |
| PVA20SP | 130 | $1.73 \times 10^{-7}$ | |
| PVA40SP | – | $4.08 \times 10^{-6}$ | 0.87 |
| PVA40SP | 110 | $2.09 \times 10^{-6}$ | 0.53 |
| PVA60SP | – | $5.34 \times 10^{-6}$ | 0.91 |
| PVA60SP | 130 | $4.84 \times 10^{-7}$ | 0.37 |
| Nafion 117 | | $2.80 \times 10^{-6}$ | 0.82 |

Table 2 summarizes the IEC, water uptake, conductivity values for samples containing 20, 40, 50, 60 and 80 wt.% s-Ph and some samples cured at 110 and 130 °C. For convenience of discussion, the monomer mole ratio for s-PH and vinyl alcohol calculated from the weight fraction is also included in parentheses in the first column.

Based on a simple geometric calculation from the size of the monomer (the separation between adjacent sulfonate groups is 5.5 Å, and for vinyl alcohols, it is 1.9 Å) and by assuming a stretched conformation, it is estimated the pairing of sulfonate phenolic and vinyl alcohol monomers occurs at a 1:3 mole ratio, where the "polymer-complex" can be formed, i.e. the sulfonate from s-Ph is forming hydrogen bonding with every fourth PVA unit in the fully stretched arrangement. It is highly plausible that a single s-Ph chain can pair with a multiple PVA chain. The ratio when the polymer-complex occurs may be smaller since the chains are not fully stretched. Although this calculation is approximate, it can be expected that the sample PVA60SP bears the closest composition to the polymer-complex. Direct evidence of such "polymer-complex" formation is derived from the TGA results, which shows PVA60SP that bears the highest decomposition temperature near 550 °C. When the amount of either s-Ph or PVA exceeds this mole ratio, the system will consist of isolated s-Ph or isolated PVA domains, in addition to the "polymer-complex". It becomes interesting to examine how the change of polymer composition, which alters the fractions of three domains, can influence the proton conductivity, and methanol permeation.

Table 3 shows that the water uptake and IEC value increase with increase of s-Ph concentration. However, λ (the number of water molecules available per sulfonate group) value decreases with increasing s-Ph concentration and is lowest at the 3:1 ratio composition (PVA60SP) where the "polymer-salt" is expected. In this case, complete acid–base pairing has prevented high solvent uptake, but the chain mobility is still sufficient to support proton transport. In addition, the full miscibility also prevented the formation of localized water clusters that have no access to acidic sulfonate groups (thus not contributing towards conduction). This is the case when PVA is in excess (PVA20SP, PVA40SP), where λ is high but fewer protons are available for conduction. On the other hand, in PVA80SP when s-Ph is in excess, the IEC approaches 2.66 mmole $g^{-1}$, the λ value again increases substantially and the proton conductivity is also high. In this case, however the substantial water uptake weakens the membrane. These important results suggest that proton transport in an aqueous environment can be activated by less than 40 water molecules surrounding each sulfonate group (the lower limit of water is not yet determined). It also raises the point that for a properly structured conduction environment and channel connectivity (e.g. by forming the polymer-complex), a favorable proton transport condition is achieved by the least amount of water. For the pure s-Ph sample (IEC value exceeds 3.1), the membrane swells severely in water and the conductivity cannot be measured correctly.

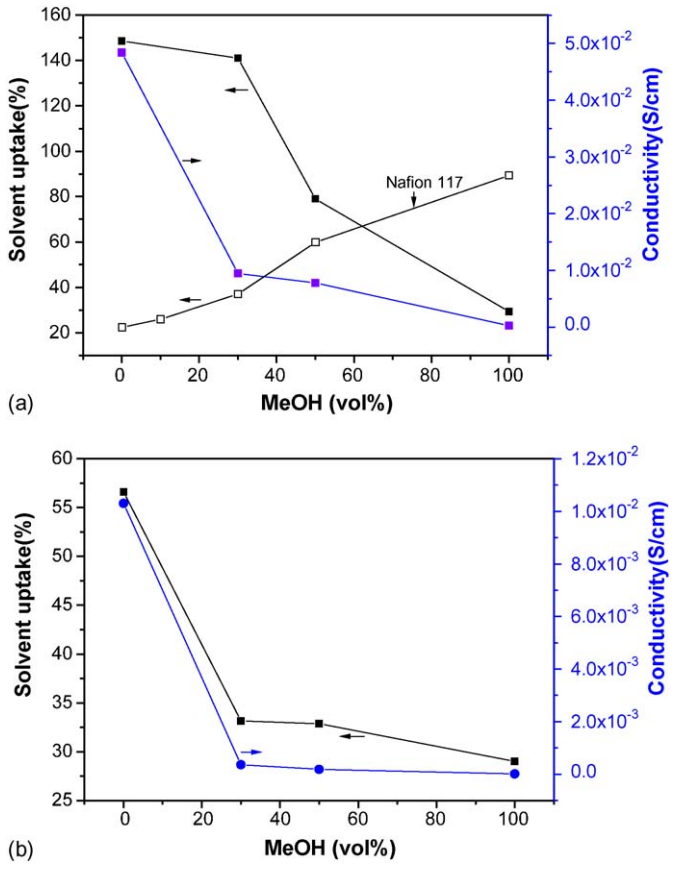


Fig. 6. Solvent uptake and conductivity at different methanol vol.% for (a) PVA60SP and (b) PVA60SP cured at 130 °C.

The membrane faces the greatest challenge in a concentrated methanol solution, where the possibility of swelling weakens the membrane properties and the crossover effect limits its function in DMFCs [21–23]. Fig. 6a and b show the variation of the solvent uptake as a function of methanol concentration for the PVA60SP membrane before (Fig. 6a) and after (Fig. 6b) curing at temperature of 130 °C. The solvent uptake data for Nafion 117 are also included in Fig. 6a for comparison. As observed from Fig. 6a, the swelling ratio decreases from 150 to 130% with an increase in methanol concentration. Although the conductivity is also decreased, the value is of the order of $10^{-2}$ S $cm^{-1}$. In comparison with Nafion 117, a severe swelling to about 100% can be found with increasing methanol concentration, where it no longer is a free-standing film.

Contraction of the cross-linked matrix with increasing methanol content, and thus the reduced methanol permeabil-

ity compared to that with the conventional Nafion membrane, is a valuable property of the present membrane. With these merits, the material is applied not only to fuel cells but also to separation membranes and applications in concentrated alcohol conditions. In the case of Nafion, methanol shows a higher affinity with the ether groups of the side chains, and gradually dissolves into the otherwise hydrophobic PVdF or PTFE backbone. In the case of an aromatic side chain, the solubility parameter of the aromatic group is different from that of methanol, and repels the uptake of methanol, compared to that of water. NMR quantification indicated that the composition of methanol inside the membrane is less than that in the solution and suggests that the membrane favors water uptake over methanol. This is contrasted with Nafion where the methanol concentration remains about the same in the membrane as it is in the fuel stream. For the membrane cured at 130 °C (Fig. 6b), the covalently cross-linked structure has effectively reduced the methanol uptake. At 30 vol.% methanol, the solvent uptake falls to around 32%. The proton conductivity dropped to below the $10^{-3}$ S cm$^{-1}$ level.

Table 3 summarizes the results including the methanol permeability for samples containing a different wt.% of s-Ph and curing at 110 and 130 °C. With increasing s-Ph, the methanol permeability increased slightly. But after curing, the permeability dropped one order from $10^{-6}$ to $10^{-7}$ cm$^2$ s$^{-1}$, which suggested that cross-linking has effectively reduced methanol permeation. However, the proton conductivity is also reduced. The last column of Table 3 indicates that the conductivity/permeability ($\sigma/P$) ratio is higher for membranes without curing, which suggests cross-linking has suppressed more conductivity than methanol permeation. The two samples PVA40SP and PVA60SP where the polymer-complex is most abundant, displayed the best balance between high proton conductivity and low methanol permeation. In both cases, the $\sigma/P$ ratio was higher than Nafion.

## 4. Conclusions

Although far from being ideal for a membrane for fuel cell applications, the current results unveil a plausible structural design employing both a proton donor polymer and a proton acceptor polymer. The membranes composed of s-Ph acid and PVA base displayed good proton conductivity, of the order of $10^{-2}$ S cm$^{-1}$ at ambient temperatures. Upon cross-linking above 110 °C, covalent links between PVA and s-Ph were established. Although this sacrificed a certain amount of sulfonate groups, leading to a slight reduction of proton conductivity, this conductivity value was still at the $10^{-2}$ S cm$^{-1}$ level. In sharp contrast to Nafion, and other polymer electrolytes disclosed in the literature, the current membrane (both before and after cross-linking) showed a reduction of methanol solvent uptake with increasing methanol concentration. These films have been found to show a permeability of $10^{-7}$ cm$^2$ s$^{-1}$ with increase of s-Ph concentration and with increasing curing temperature. The low methanol cross-over (lower methanol permeation value) is attributed to the reduced solvent uptake as well as to the higher membrane selectivity towards water. Although both methanol permeation and proton conductivity are lower compared to Nafion, the conductivity/permeability ratio of 0.97 for the PVA/s-Ph 40:60 composition is actually higher than that determined for Nafion. The results illustrate the importance of tailoring the structure of a proton conduction channel (in the present case, by formation of a polymer-complex) when high proton conductivity can be realized with less water. Such a structure is also effective in reducing methanol uptake where the swelling ratio decreases with increase of methanol concentration. Contraction of the cross-linked matrix with increasing methanol content, and thus the reduced methanol permeability compared to that with the conventional Nafion membrane, is a valuable property of the present membrane.

## Acknowledgment

National Science Council provides funding to carryout this research work under the contract no. NSC 93–2811–M 008–017.

## References

[1] K.D. Kreuer, Solid State Ionics 136 (2000) 149–160.
[2] A. Noda, Md.A.B.H. Susan, K. Kudo, S. Mitsushima, K. Hayamizu, M. Watanabe, J. Phys. Chem. B 107 (2003) 4024–4033.
[3] K.D. Kreuer, J. Membr. Sci. 185 (2001) 29–39.
[4] M. Yamada, I. Honma, Electrochim. Acta 50 (2005) 2837–2841.
[5] K.D. Kreuer, Chem. Mater. 8 (1996) 610.
[6] H.G. Herz, K.D. Kreuer, J. Maier, G. Scharfenberger, M.F.H. Schuster, W.H. Meyer, Electrochim. Acta 48 (2003) 2165–2171.
[7] J.T. Wang, J.S. Wainright, R.F. Savinell, M. Litt, J. Appl. Electrochem. 26 (1996) 751.
[8] J.S. Wainright, J.T. Wang, R.F. Savinell, M. Litt, H. Moaddel, C. Rogers, Extended Abs., The Electrochem. Soc. Spring Meeting, San Francisco 94 (1994).
[9] M. Yamada, I. Honma, Chem. Phys. Chem. 5 (2004) 724–728.
[10] M. Yamada, I. Honma, Electrochim. Acta 40 (2003) 2411–2415.
[11] J. Kerres, A. Ullrich, F. Meier, T. Haring, Solid State Ionics 125 (1999) 243–249.
[12] J. Kerres, W. Cui, US Patent No. 6,300,381 (2001).
[13] J. Kerres, W. Cui, US Patent No. 6,194,474 (2001).
[14] J. Kerres, W. Cui, W. Zhang, J. Polym. Sci: Part A: Polym. Chem. 36 (1998) 1441–1448.
[15] J.A. Kerres, J. Membr. Sci. 185 (2001) 3–27.
[16] W. Zhou, M. Yoshino, H. Kita, K. Okamoto, J. Membr. Sci. 217 (2003) 55–67.
[17] J. Qiao, T. Hamaya, T. Okada, Chem. Mater. 17 (2005) 2413–2421.
[18] D.H. Jung, S.Y. Cho, D.H. Peck, D.R. Shin, J.S. Kim, J. Power Sources 106 (2002) 173–177.
[19] P.P. Chu, H.-D. Wu, Polymer 41 (2000) 101–109.
[20] C. Vogel, J. Meier-Haack, A. Taeger, D. Lehmann, Fuel Cell 4 (2004) 320–327.
[21] Q. Li, R. He, J.O. Jensen, N.J. Bjerrum, Chem. Mater. 15 (2003) 4896–4915.
[22] T. Ioroi, K. Kuraoda, K. Yasuda, T. Yazawa, Y. Miyazaki, Electrochem. Solid-State Lett. 7 (2004) A394–A396.
[23] A.S. Arico, V. Baglio, P. Creti, A. Di Blasi, V. Antonucci, J. Brunea, A. Chapotot, A. Bozzi, J. Schoemans, Power Sources 123 (2003) 107–115.